Talanta 166 (2017) 27–35

Contents lists available at ScienceDirect

Talanta

journal homepage: www.elsevier.com/locate/talanta

DNA-wrapped multi-walled carbon nanotube modified electrochemical biosensor for the detection of Escherichia coli from real samples

Dilsat Ozkan-Ariksoysal[a,*], Yasin Ugur Kayran[a], Fethiye Ferda Yilmaz[b], Anton Alexandru Ciucu[c], Iulia Gabriela David[c], Vasile David[c], Mine Hosgor-Limoncu[b], Mehmet Ozsoz[a]

[a] Department of Analytical Chemistry, Faculty of Pharmacy, Ege University, 35100 Bornova, Izmir, Turkey
[b] Department of Pharmaceutical Microbiology, Faculty of Pharmacy, Ege University, 35100 Bornova, Izmir, Turkey
[c] Department of Analytical Chemistry, Faculty of Chemistry, University of Bucharest, 90-92 Panduri Avenue, District 5, 050663 Bucharest, Romania

ARTICLE INFO

Keywords:
Electrochemical DNA biosensor
DNA-wrapped multi-walled carbon nanotubes
Pencil graphite electrode (PGE)
Escherichia coli detection
DNA Hybridization
Polymerase chain reaction (PCR) amplified real samples

ABSTRACT

This paper introduces DNA-wrapped multi-walled carbon nanotube (MWCNT)-modified genosensor for the detection of Escherichia coli (E. coli) from polymerase chain reaction (PCR)-amplified real samples while Staphylococcus aureus (S. aureus) was used to investigate the selectivity of the biosensor. The capture probe specifically recognizing E. coli DNA and it was firstly interacted with MWCNTs for wrapping of single-stranded DNA (ssDNA) onto the nanomaterial. DNA-wrapped MWCNTs were then immobilised on the surface of disposable pencil graphite electrode (PGE) for the detection of DNA hybridization. Electrochemical behaviors of the modified PGEs were investigated using Raman spectroscopy and differential pulse voltammetry (DPV). The sequence selective DNA hybridization was determined and evaluated by changes in the intrinsic guanine oxidation signal at about 1.0 V by DPV. Numerous factors affecting the hybridization were optimized such as target concentration, hybridization time, etc. The designed DNA sensor can well detect E. coli DNA in 20 min detection time with 0.5 pmole of detection limit in 30 μL of sample volume.

1. Introduction

Electrochemical DNA biosensors have been developed over the past decades for various research purposes in many fields including gene diagnosis, environmental monitoring, etc. They have some powerful benefits such as they are label-free and the electrochemical transduction is more rapid and direct [1] than other optical or piezoelectric detection methodologies. Still, the need for simple and sensitive portable devices for the detection of specific DNA sequences, biosensor design technologies have continuously improved along with the advancements in nanoscience.

Bacteria are widely spread on the earth and many of their species responsible for infectious diseases such as *Escherichia coli*, Salmonella spp., Shigella spp., Vibrio spp., Listeria monocytogenes, Staphylococcus aureus, Bacillus cereus, Clostridium perfringens, Campylobacter jejuni, and Legionella spp.[2] Among them, S. aureus [3] and E. coli [4], in general are the most common causative agents of food and waterborne diseases. S. aureus often causes many infections such as, pneumonia, pseudomembranous colitis, pericarditis, sepsis and food poisoning by staphylococcal enterotoxins [3]. E. coli usually leads to gastrointestinal complaints such as nausea, vomiting, diarrhea, and renal and hepatic problems in severe cases [4].

The detection of microorganisms has been carrying out for ages by traditional culturing methods, PCR and ELISA. These conventional methods achieve the detection successfully however they are time consuming or expensive techniques [2,5]. However, alternative techniques such as electrochemical and optical biosensors have great interest lately due to their high specificity and short measurement times [5]. Biosensor studies also provide a development of affordable methods for elicitation of bacteria from clinical, water, food, and environmental samples for various organisms [2–4].

Nanomaterial-based biosensors have been preferred for ultrasensitive DNA analysis in recent years, because the only limitation especially for electrochemical transducers is the limit of detection that is far from optical devices. Among them, carbon nanotube(CNT)-based transducers have still received considerable attention and many of electrochemistry-based works have been published related to advantages of CNTs [6,7]. Particularly, CNTs have been used in biosensors to obtain high sensitivity from the sensing surface via two basic principles. One of them is CNTs provide excellent conductivity, therefore, CNTs-modified sensors give an enhanced output signal in comparison to unmodified ones. Second is that the immobilization of high amount of

* Corresponding author.
E-mail address: dilsat.ariksoysal@ege.edu.tr (D. Ozkan-Ariksoysal).

http://dx.doi.org/10.1016/j.talanta.2017.01.005
Received 23 October 2016; Received in revised form 30 December 2016; Accepted 3 January 2017
Available online 10 January 2017

biomolecules onto the CNTs is possible via self-assemble strategy, so it is quite easy to obtain enhanced surface area and increased response [8–11].

More recently, many of research groups have focused on functional hybrid assemblies related to CNT-biomaterial(e.g., protein, enzyme, antibody, antigen, nucleic acids) hybridization in the field of biosensors for biomedical applications [12]. In these hybrid structures, while CNTs provide conductive or semi-conductive properties, biomolecule provides recognition or catalytic activity in general [13]. The integration of biomaterials with CNTs is also important in healthcare field, because modified CNTs are able to pass through the cell membrane easily without cytotoxicity [14]. Therefore, CNTs can be used as special carriers for the transport of biomolecules into cells.

On the other hand, there have been growing interest in hybrid materials of DNA and carbon nanotubes because while CNTs have many of electrical and physical properties, their poor aqueous solubility could still be a problem for applications. The solubility of DNA-CNT nanohybrid structure was first reported in 2003 by Zheng et al. [15] and they reported ss-DNA could wrap on the CNTs as a complex structure if CNTs sonicated with DNA in a suitable conditions. While DNA molecule can wrap around a nanotube via noncovalent π–π stacking interaction between the nitrogen bases of DNA and nanotube, the phosphate backbone of DNA strand (hydrophilic section) in through the water solution. CNT-DNA complexes also protect their stability due to the π-stacking [16]. In the same year, Nakashima et al. were also presented increased solubility of single-walled carbon nanotubes with double-stranded DNA (ds-DNA) in aqueous media independently [17]. The formation mechanism of DNA-CNT hybrids is not clear completely yet, but their good solubility [18–20] have great potential for development of new analytical techniques related to nanomaterial-based DNA analysis.

DNA-functionalized CNTs are generally used for dispersion analysis. For example, Hughes et al. reported the interaction between 15-mer polynucleotide sequences as polyadenine, polyguanine, polycytosine or polytyhmine and CNTs and they found the dispersion efficiency of CNTs in the presence of these polynucleotides [21]. Additionally, dsDNA, ssDNA and other short-length nucleic acids have been used for that purpose [22,23]. There have also been efforts made to chemical characterization of ssDNA-CNTs hybrid structures [12]. Thus, the chemistry of DNA-CNTs complexes have been studied more than those of their biological applications.

In biosensor field, Aravind et al. reported the detection of dopamine by using ssDNA-wrapped MWCNTs recently [24]. A sensitive immunosensor was developed by Cao et al. for the detection of human chorionic gonadotrophin by dsDNA-functionalized MWNTs, methylene blue and glassy carbon electrode(GCE) [25]. Shi et al. demonstrated microbiosensors for the detection of glucose and ATP using ssDNA-SWNT complex [26]. In another study, single base mismatch detection was performed by Zhang et al. by using label-free analysis strategy based on light scattering signals [27]. Williams et al. found inhibitory concentration of DNA-SWCNTs complexes in PCR [28]. Many of other biosensor reports related to DNA-wrapped CNTs have been reviewed by Kazuo Umemura comprehensively [12]. Besides, some interesting applications related to DNA-decorated CNTs were presented in the field of electro-analytical chemistry. Thuy et al. studied about the sequence-specific DNA detection related to the E. coli O157:H7 and they prepared ssDNA-wrapped MWCNTs for the immobilization of the interdigitated microelectrode. The developed biosensor detected 1 nM synthetic target DNA in 10 min response time based on potential measurements [20]. Jiao and coworkers reported a label-free GCE-containing biosensor for the detection of DNA hybridization based on the guanine signal in 45 min hybridization time. A low limit of detection was found as 20 nM for synthetic target oligonucleotide [29]. In another study performed to determine hepatitis B virus DNA [30], the DNA-CNTs structures were used as sensitive electrochemical label. In that study, a sandwich hybridization method was preferred which containing a signaling probe wrapping around the nanomaterial and a capture probe modified on the magnetic beads.

In the present study, by using the excellent properties of ssDNA-MWCNTs hybrid structure, we propose the application of DNA-wrapped multi-walled carbon nanotube for the detection of E. coli from polymerase chain reaction amplified real samples (traditional PCR and asymmetric PCR) for the first time. There is no report about "real sample analysis" by using DNA-wrapped MWCNTs, PGE and YES/NO detection system in the literature. The properties of ssDNA-decorated CNTs system was evaluated comprehensively and major parameters of the designed biosensor was characterized. The analytical performance of the developed biosensor was discussed along with future prospects in the further sections.

2. Material and methods

2.1. Apparatus, chemicals and sample preparation

DPV signals were monitored via AUTOLAB 12 potatiostat/galvanostat electrochemical analyzer system purchased from Eco Chemie, Netherlands. by using pencil graphite electrodes (PGEs). The raw voltammogram was smoothed by Savitzky and Golay filter (level 2) of GPES software. Three electrode system contains PGE which is 3 cm of graphite rod (0.5 mm diameter) as a working electrode (Tombo, Japan), a reference electrode (Ag/AgCl) and a platinum wire as an auxiliary electrode. A rotring model pencil was used as a holder for PGEs.

All electrochemical measurements were carried out in 0.50 M Acetate buffer solution (ABS). The raw voltammograms were treated by using the Savitzky and Golay filter (level 2) included in the General Purpose Electrochemical Software (GPES) of Eco Chemie with moving average baseline correction, using a "peak width" of 0.01 V. Raman NRS-3100 Spectroscopy JASCO device was used for monitoring of Raman signals.

Buffers and their contents used in this work are explained in Table 1. Single and multi walled –COOH functionalized carbon nanotubes powders were supplied from Dropsense (Spain). Chitosan and other chemicals (buffers, etc.) were purchased from Merck and Sigma as an analytical grade. Ultrapure water (18Ω) was used in all solutions (Elgastat, England). All experiments were carried out at room temperature (22.0–25.0 °C).

2.2. DNA materials

Target sequences were determined based on conserved regions in bacterial 16S rDNA for E. coli [31,32] and species specific Sa442 genomic DNA fragment for S. aureus [33]. The 16-mer synthetic inosine-substituted E. coli-specific probes and their guanine-containing complementary targets were supplied from TIB MOLBIOL (Germany) as lyophilized powder. The inosine base is the analogue of guanine and it is electro inactive at about 1.0 V. The base sequences of the oligonucleotides are listed in Table 2.

1000 μg/mL stock solutions of synthetic oligonucleotides and PCR samples were kept at −20 °C until to use. The detailed amplification

Table 1
Buffers and their contents used in this study.

Buffer type	Contents
Pretreatment and measurement buffer	**ABS;** 0.50 M acetic acid and 20 mM NaCl (pH:4.8)
Preparation buffer for dilution of DNA oligonucleotides, washing and hybridization buffer	**PBS;** 0.01 M KH_2PO_4, 0.04 M K_2HPO_4 and 20 mM NaCl (pH 7.4)
Preparation buffer for stock solutions of oligonucleotides	**TE;** 10 mM Tris-HCl, 1 mM EDTA (pH 8.00, TE

Table 2
Abbreviations and base sequences of synthetic oligonucleotides.

Name	Sequences (16 bp length)
E. coli target	5′-GGC CTT CGG GTT GTA A-3′
E. coli probe	5′- **NH2**-TTA CAA CCC IAA IIC C-3′
S. aureus target	5′-AAC GCT CAT TCG CGA T-3′
S. aureus probe	5′- **NH2**-ATC ICI AAT IAI CIT T-3′

procedure for conventional or asymmetric PCR was explained below.

2.2.1. PCR amplification

Real DNA fragments related to E. coli and S. aureus were amplified with conventional PCR and asymmetric PCR methodologies provided from Ege University Faculty of Pharmacy Department of Pharmaceutical Microbiology.

Template genomic DNA extracted from S. aureus ATCC 25923 and E. coli ATCC 25922 by boiling lysis method. PCR amplification was performed in 50 μL total volume with 16S rRNA universal primers (E341F: 5′-CCT ACG GGA GGC 5GC A-3′; E533R: 5′-T5C CGC 55C T5C TGG CAC-3′; 5: Inosin) to produce a 192-bp amplicon from E. coli genomic DNA and species specific primers (Sa442-1: 5′-AAT CTT TGT CGG TAC ACG ATA TTC ACG-3′; Sa442-2: 5′-CGT AAT GAG ATT TCA GTA GAT AAT ACA ACA-3′) to produce a 108-bp amplicon from S. aureus genomic DNA. PCR reaction mixture contained 1.25 U of Taq DNA polymerase (Fermentas), 1.5 mM MgCl2, 200 μM each deoxynucleoside triphosphate, 30pmol of each primer and 30–40 ng of template DNA. The mixture was exposed to following thermal cycling program; 5 min initial denaturation at 95 °C, and then 30 cycles of 1 min denaturation step at 94 °C, 1 min annealing 57 °C and 45 °C for S. aureus and E. coli, respectively, 1 min elongation at 72 °C, and a final extension of 10 min at 72 °C with a TC-312 thermal cycler (Techne Inc., Burlington, USA). PCR products were loaded a 1.5% (w/v) agarose gel, after electroporation they were stained with ethidium bromide and confirmed under UV light. Asymmetric PCR (aPCR) samples were produced by using the same primers. However, ratios of them were set to 100:1 in the reaction mixture.

2.3. Methods

The experimental protocol included (i) Preparation of MWCNTs and probe-DNA-decorated MWCNTs, (ii) construction of the PGE surface for hybridization and (iii) detection of hybridization and DPV monitoring of current signals were illustrated in Scheme 1.

2.3.1. Hybridization control of synthetic oligonucleotides by using gold standard method "agarose gel electrophoresis"

The hybridization ability of synthetic oligonucleotides related to E. coli and S. aureus DNA sequences were checked out by using gel electrophoresis method (Fig. S1, see Supplementary file).

2.3.2. The functionalization of nanotubes with E. coli or S. aureus-specific probe

1 mg/mL of –COOH group functionalized MWCNT was suspended in ultrapure water and sonicated during 4 h at room temperature. The sonication process is an important step for effective dispersion of MWCNTs in water [20]. Inosine (I)-substituted and amino(-NH_2)-tagged capture probe was added into the nanotube suspension (final concentration 7 μg/mL) immediately and mixed with MWCNTs by using a shaker [29] at 600 rpm for 30 min at 30 °C. During this time, probe DNA interacted with MWCNT and wrapped on CNT via π-stacking interactions [15].

2.3.3. Preparation of the sensor surface

Disposable PGEs were pretreated by applying a potential of +1.40 V for 30 s in acetate buffer (ABS;pH 4.80). Each pretreated PGE was immersed into the vials containing 30 μL of probe DNA-wrapped CNTs solution during 1 h for the preparation of PGE surface via wet adsorption method [34]. Besides this, possible covalent or electrostatic (van der Waals forces) interactions can happen on PGE between –COOH containing pretreated surface and amino-tagged capture probe which wrapped on MWCNTs. These issues have been reported previously [35,36]. Probe modified electrodes were then washed with phosphate buffer (PBS;pH 7.40) for three times during 5 s to remove unbound nanohybrids from the PGE surface. Due to the phosphate backbone of the probe DNA, sensor surface was negatively charged after the immobilization of the nanohybrid structure.

2.3.4. Chitosan interaction with the nanohybrid modified PGE

5 mg amount of chitosan was dissolved in glacial acetic acid (1%) to obtain saturated chitosan solution (pH:5.0) and it filtered by using filter paper to remove the excessive amount of chitosan. The DNA-MWCNTs nanohybrid modified PGEs were immersed into the eppendorf tubes that containing 50 μL of saturated chitosan solution for 45 min. PGEs were then rinsed with PBS for 5 s to minimize nonspecific chitosan adsorptions on the electrode surface.

Chitosan has an important role to increase the stability of the designed sensor. For this purpose, the negatively-charged nanohybrid modified PGE was interacted with positively charged chitosan before the hybridization. Chitosan molecule has cationic nature and thus, it can form a stable polyion complex with negatively charged DNA [37]. It can also bind to the carbon nanotubes to construct an another stable complex with them and it increases the sensitivity of DNA detection [38,39]. The aggregation and saturation of nucleic acids on chitosan modified CNTs and increasing the conductivity of chitosan with MWCNTs were identified by Ensafi's group [40]. In an another literature, chitosan molecule was used not only for the stabilizing of single stranded (probe) DNA but also double strand (hybrid) DNA [41]. Additionally, Zhang et al. and Jung et al. showed that the desorption of double stranded DNA from CNT surface after the hybridization [29,42]. However, there have not been any literature related to chitosan immobilization onto the probe-DNA covered sensor similarly with our procedure. As a result, this is the first study in this field and we prefer to use chitosan as a "stabilizing layer" for the construction of the sensing layer.

2.3.5. Hybridization and voltammetric transduction of modified PGEs

The capture probe-wrapped MWCNTs-immobilized PGEs were dipped into the 12 μg/mL concentration of synthetic target solution after the surface treatment of chitosan. The hybridization was allowed to proceed for 20 min at room temperature and the negatively charged target DNA was then easily and effectively hybridized with probe DNA on the partly neutralized PGE surface by chitosan. After the hybridization, graphite lead was then immersed into PBS for 5 s by stirring to remove unbound sequences from the surface. The same procedure was also used for the detection of probe-noncomplementary and probe-PCR interactions in order to control selectivity of the biosensor.

PCR-amplified real samples produced from E. coli or S. aureus gene region by using typical PCR method were diluted with PBS(dilution rates are 1:50 and 1:100) and were then put into tubes for denaturation (heated at 96 °C for 7 min in a PCR machine and immediately 0 °C for 2 min in ice bath.) DNA-MWCNTs nanohybrid modified PGEs were rapidly dipped into the eppendorf tubes that containing denatured PCR samples. The hybridization reaction between probe and amplified product occurred in 20 min at room temperature. After that the modified electrodes were washed with PBS for 5 s by stirring to minimize nonspecific adsorptions to the sensor surface.

The asymmetric PCR technique was also used in this study to obtain single strand and high amount of target DNA. For this purpose, before the amplification, the ratio of primers were set to 100:1 in the reaction

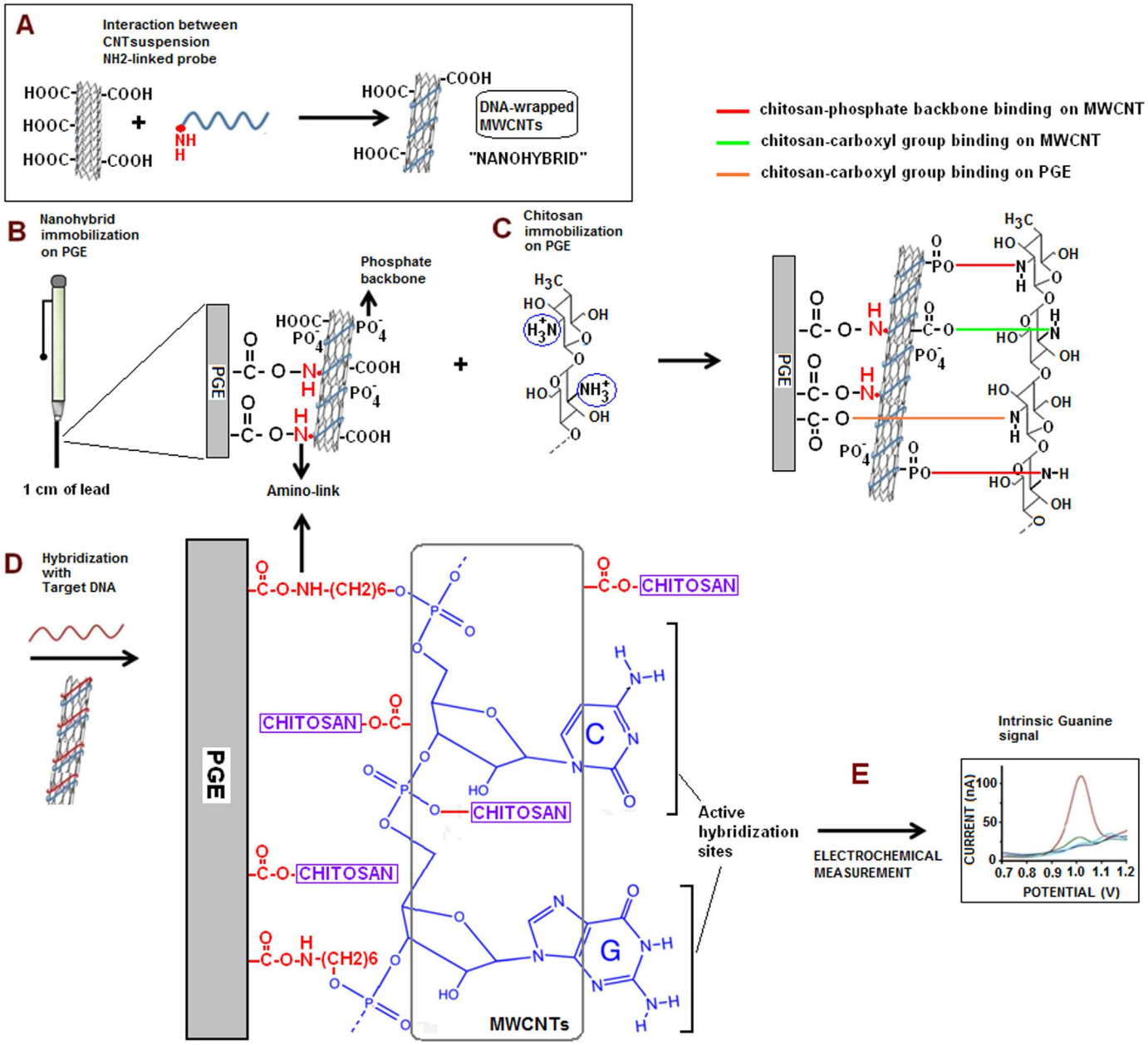

Scheme 1. The assay involved five steps: The interaction between –COOH functionalized MWCNTs and $-NH_2$ linked capture DNA(A), immobilization of the nanohybrid material onto PGE(B), chitosan immobilization on the DNA-wrapped CNT-modified PGE(C), hybridization(D) and DPV measurement of guanine oxidation signal(E).

mixture; thus, the concentration of specific target section was obtained 100 times higher than the other PCR chain. Consequently, after the asymmetric PCR reaction, product obtained was used directly in the experiment as a real target without denaturation process.

DPV technique was used for the measurement of intrinsic guanine signal at about +1.00 V stem from hybridization between inosine-substituted probe and its complementary target. The appearance of the highest guanine oxidation signal proves the hybridization of surface DNA with the full-match target sequence, whereas no guanine response is observed from probe DNA. (YES/NO detection system).

The oxidation signal of guanine was measured in blank ABS before and after hybridization by scanning from +0.70 to +1.45 V with the amplitude of 50 mV at 16 mV/s scan rate. Repetitive measurements related to hybridization were carried out by using only DNA and DNA-wrapped MWCNTs modified PGEs. The non-complementary sequence related to S. aureus was used for the detection of biosensor selectivity.

3. Results and discussion

Initially, the hybridization control of synthetic oligonucleotides by using agarose gel electrophoresis and the characterization of DNA-wrapped carbon nanotubes by Raman Spectroscopy were studied respectively. Next, optimum experimental conditions of the developed genosensor were determined. Finally, the electrochemical detection of E. coli DNA was detected clearly. Comprehensive experiments carried out in this study and their topics are summarized in Table 3 for clarity.

3.1. Characterization of DNA-wrapped carbon nanotube by Raman Spectroscopy

Raman spectroscopy is one of the powerful technique for the characterization of carbon-based materials. According to the literature [43], D-band and G-band in the Raman spectrum of carbon structures correspond to carbon stretching modes of sp^2 and sp^3 respectively. In

Table 3
Complementary experiments carried out in this study.

Figure number	Figure's description
Fig. S1	Hybridization control of synthetic oligonucleotides used in this work by the gold standard method “agarose gel electrophoresis”
Fig. 1	Characterization of DNA-wrapped carbon nanotube by Raman Spectroscopy
Fig. S2	The effect of chitosan on hybridization and biosensor selectivity.
Fig. 2	The effect of DNA-wrapped carbon nanotube modification on the biosensor response
Fig. S3	Optimum probe DNA concentration for wrapping of MWCNTs.
Fig. 3	Hybridization and selectivity tests by using different types of CNTs.
Fig. 4	Detection Sensitivity(Target concentration study).
Fig. S4	The effect of wrapping time of the capture probe onto MWCNT on hybridization and biosensor selectivity.
Fig. S5	The effect of chitosan concentration on hybridization a and biosensor selectivity.
Fig. S6	The effect of chitosan-PGE interaction time on hybridization.
Fig. S7	The effect of the nanohybrid immobilization time onto PGE surface on hybridization signal.
Fig. 5	The analysis of typical PCR products.
Fig. 6	The analysis of asymmetric PCR samples.

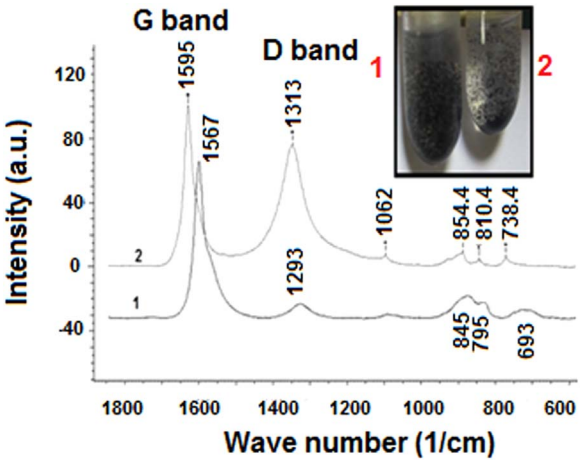

Fig. 1. The photograph represents the solubility of CNTs in ss-DNA contained aqueous media. Comparison of Raman spectra of MWCNTs (1) and NH_2-tagged probe DNA-wrapped MWCNTs modified (2) PGEs.

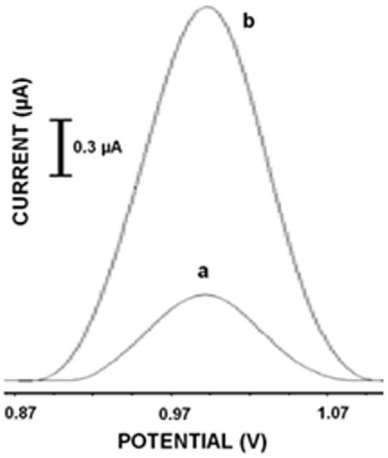

Fig. 2. Influence of DNA-wrapped MWCNTs-modification on the sensitivity of biosensor by using guanine-contained E. coli target DNA. DPV of guanine oxidation signals obtained from (a) only DNA-modified and (b) DNA-wrapped MWCNTs-modified electrodes. The required amount of CNTs mixed with DNA during 30 min. Immobilization of DNA-CNTs hybrid on PGE for 1 h. Interaction between chitosan solution and modified PGEs for 45 min. Measurement in ABS.

Fig. 1, the wrapping of DNA on MWCNTs was demonstrated by a photograph and the characterization of the structure was monitored by Raman spectroscopy. In the photograph, it is clearly seen that the solubility of CNTs increased when the DNA sequence interacted and wrapped with MWCNTs in aqueous media. The Raman spectrum of MWCNTs(1) and probe DNA-decorated MWCNTs(2) showed characteristic peaks at about 1300 and 1600 cm^{-1} were identified. However, a band shift was observed at about 1600 cm^{-1} in the presence of DNA(2). A possible cause for the shift in G band from 1567 cm^{-1} to 1595 cm^{-1} (28 cm^{-1}) is that the charge transfer between the DNA and MWCNTs [44]. An another explanation responsible for this downshift may be a compressive stress induced in the MWCNTs because of the DNA wrapping on the nanomaterial. Additionally, the shift in G band can also be caused by heavily functionalized nanotubes [45].

3.2. The effect of DNA-wrapped carbon nanotube modification on the biosensor response

The DNA-decorated carbon nanotube containing electrochemical genosensor can detect two types of target nucleic acids, which of one is 16-bp long synthetic DNA and one is the 192-bp of PCR amplicon obtained from E. coli or 108-bp of PCR product related to the S. aureus genomic DNA. In this study, the identification of hybridization between bacteria-specific probes and their fullmatch sequences were monitored by the appearance of the intrinsic guanine signal [46], whereas no oxidation signal of guanine was observed from inosine-contained probes (before hybridization).

DPV peak currents of guanine obtained from E. coli target DNA immobilized PGE were shown in Fig. 2. Approximately 0.60 µA of guanine response was observed from the only DNA-immobilized sensor in the absence of MWCNT. However, a signal enhancement of guanine was obtained in the presence of DNA-decorated CNT modification on PGE (The main response of guanine signal is about 1.80–2.00 µA). The magnitude of guanine signal was enhanced by 350% at DNA-wrapped MWCNTs modified PGE. The optimized experimental conditions were found as a 7 µg/mL of single-stranded DNA concentration, 30 min of DNA-wrapping on CNTs and 1 h of the nanohybrid modification onto PGE and 45 min of chitosan interaction with modified carbon transducer respectively (n=3). According to the results, the modification of PGE with DNA-wrapped CNTs allows higher surface coverage that providing enhanced DNA adsorption and thus enhanced the signal. On the other hand, enhanced signal can be caused by the high electrical conductivity of CNTs.

3.3. Hybridization and selectivity tests by using different types of CNTs

In this study, probe sequences of E. coli and S. aureus were designed with inosine-base that is the analogue of guanine and it is electro inactive at about +1.00 V [46,47]. This property brings an advantage to our approach based on a “label-free analysis” because the guanine signal is observed if the hybridization occurred on the surface of the electrode (YES/NO detection methodology). Our procedure used in the test was based on this system.

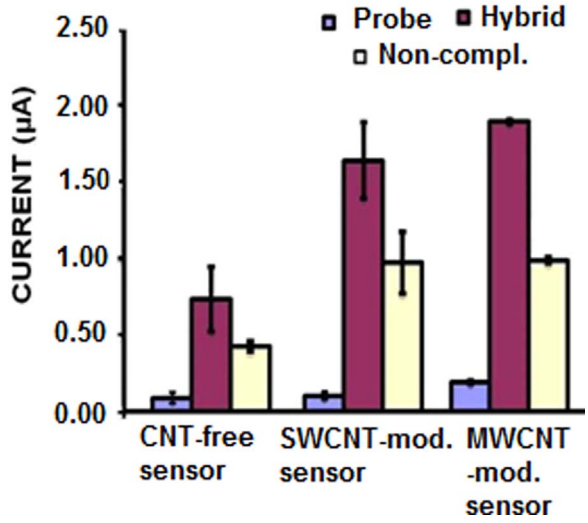

Fig. 3. The histogram related to the magnitude of guanine oxidation signal shows the effect of CNTs modifications on the sensor hybridization responses.The hybridization was occurred between probe DNA-wrapped MWCNTs and 12 µg/mL of target DNA for 20 min. Other conditions as in Fig. 2.

On the other hand, reverse control of DNA hybridization was also preferred in this work to confirm the presence of hybridization by using the guanine-contained target (E. coli or S. aureus) as a "probe" and the inosine-substituted probe as a "target" (data not shown). This control study was also aimed to show that guanine signal obtained was not caused by non-specific adsorption of target DNA onto the electrode surface directly. In that case, while the only target coated assay giving the highest guanine peak by means of available guanine bases for oxidation, the response obtained from the hybrid DNA-contained electrode showed a decline due to the hybridization between probe and target (the electrochemically active regions of guanine are partly available for oxidation). The decrease in the magnitude of the voltammetric peak of guanine thus reflected the extent of the hybrid formation (hybridization detection by using "SIGNAL DECREASE" method) [34,48,49].

Fig. 3 shows the detection of hybridization related to the E. coli DNA sequences based on guanine signal that was measured before and after hybridization between 7 µg/mL probe and 12 µg/mL complementary target. The selectivity of the capture DNA was measured by using probe to hybrid with non-specific DNA related to the S. aureus gene sequence. Nearly no oxidation signal of guanine obtained from only probe DNA-modified sensor because probe DNA does not include any guanine base. In the presence of full hybridization case, approximately 3 times higher guanine signal (Fig. 3, purple column of MWCNTs-modified sensor) was measured in comparison to the one recorded CNTs-free sensor (Fig. 3, purple column of bare sensor). It is proved that more sensitive hybridization detection was successfully achieved by using DNA-wrapped MWCNTs-modified PGE assay combined with PGE than CNT-free biosensor.

The obtained hybridization signal was approximately 2 times higher than the probe-non-complementary binding response in each modification case in Fig. 3. In other words, in the case of "non-specific binding" between probe and non-complementary sequence, nearly 50% of signal decrease was observed. Thus, the designed E. coli-specific biosensor can discriminate target and nonspecific DNA sequences.

Here it should be explained that chitosan has a critical role to increase the stability of the designed biosensor. After the hybridization, the formed dsDNA molecule also need support to stay on the MWCNT surface [29,42]. To our knowledge, this support is provided by the chitosan molecules in the vicinity. It may also reduce the hybridization rate and also cause a decrease in the selectivity. Nevertheless 50% (or more) of signal difference was obtained between complementary and noncomplementary DNA as seen in Figs. 3–6 and also in supplementary figures from S2 to S6 related to the optimum detection conditions of the developed biosensor. These results indicated that the detection of target DNA (E. coli/S. aureus) could be done selectively with the developed assay. Additionally, by using chitosan, the selectivity may be decreased insignificantly, however, a highly stable sensing layer is provided. Besides this, when chitosan was not used for the construction of the sensing surface, low and inconsistent results were obtained. In other words, target affinity of the chitosan-free assay was lower than chitosan-contained and (partially) neutralized/stabilized sensor as presented in Fig. S2, c (see Supplementary data).

On the other hand, synthetic noncomplementary oligonucleotides can bind undesirably to the capture DNA on the sensing surface because of their short length. But in real sample analysis performed with long PCR products, the signal difference between hybrid and noncomplementary DNA can be observed more clearly [34,50]. In other words, if only the sequences (Probe DNA and long PCR sample) are fully-matched, then the hybridization is form on the sensing surface. Additionally, It has also been reported in the literature that an aqueous suspension of single or multi-walled CNTs caused to the significant improvement of PCR specificity [51]. In that study, CNT nanomaterial was used as a component of PCR mixture and an apparent increase in the amount of primer binding to the template DNA was obtained, thus reducing the chances of forming non-specific PCR products. In our case, we used probe DNA-wrapped MWCNTs-modified biosensor and it can be said that PCR sequence can bind to its complementary probe sequence specifically in the presence of carbon

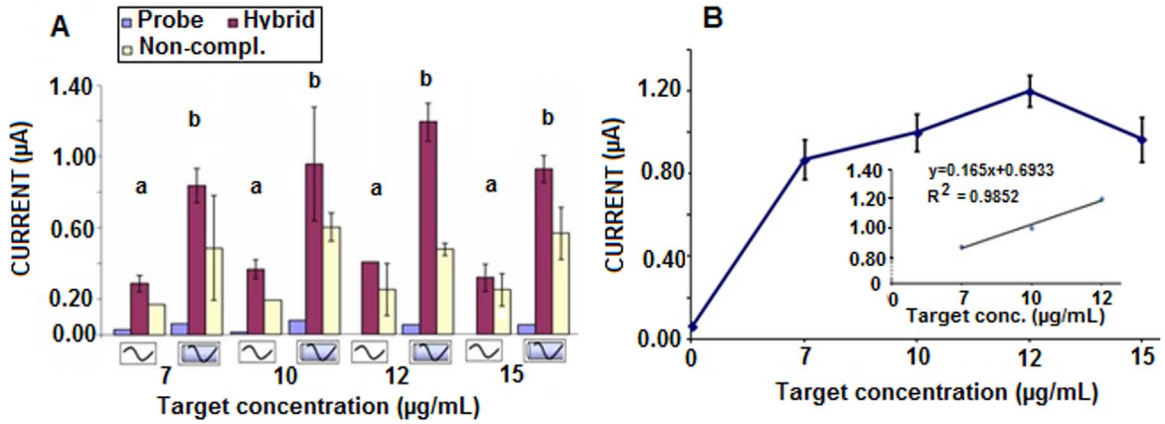

Fig. 4. (A) The effect of target DNA concentration on hybridization selectivity in the absence and presence of MWCNTs. Histogram of guanine signals which are shown as each "triple columns" obtained from (a) only DNA and (b) DNA-wrapped MWCNTs-modified electrodes that were also showed at the bottom of columns. (B) DPV signal changes of guanine obtained by using DNA-MWCNTs hybrid-modified PGEs and various concentrations of target DNA from 7 to 15 µg/mL.

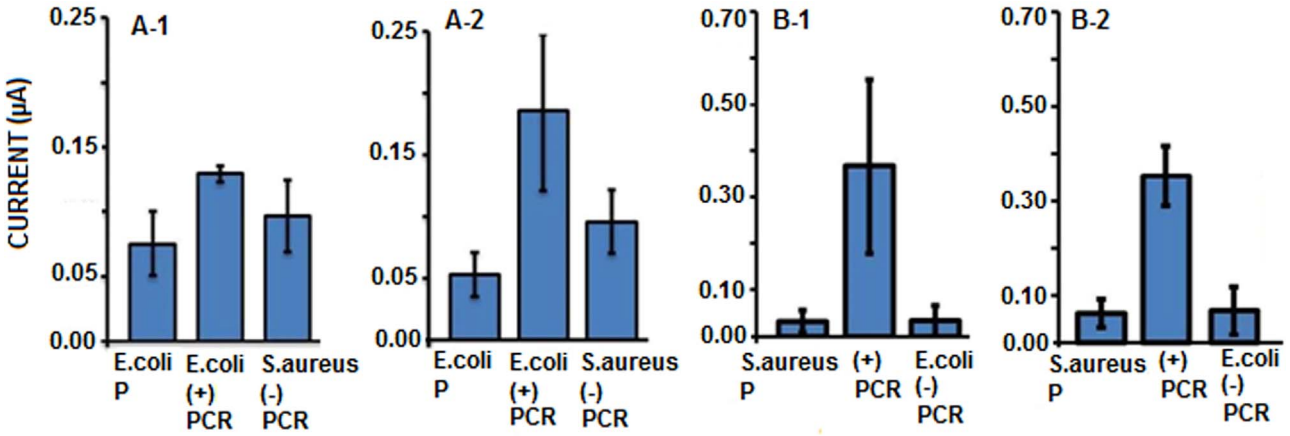

Fig. 5. Real sample analysis based on hybridization between E. coli probe (P) and E. coli PCR (Fig. 5A1 and A2); S. aureus probe (P) and S. aureus PCR (Fig. 5B1 and B2) were showed respectively with PCR dilution ratios of 1:50. A1 and B1 represent CNT-free and A2 and B2 show DNA-wrapped CNT-modified sensors. Hybridization between denatured PCR amplicon and probe on PGE was allowed for 20 min and DPV measurement was performed in ABS. Error bars show standard deviations guanine signals from three replicates.

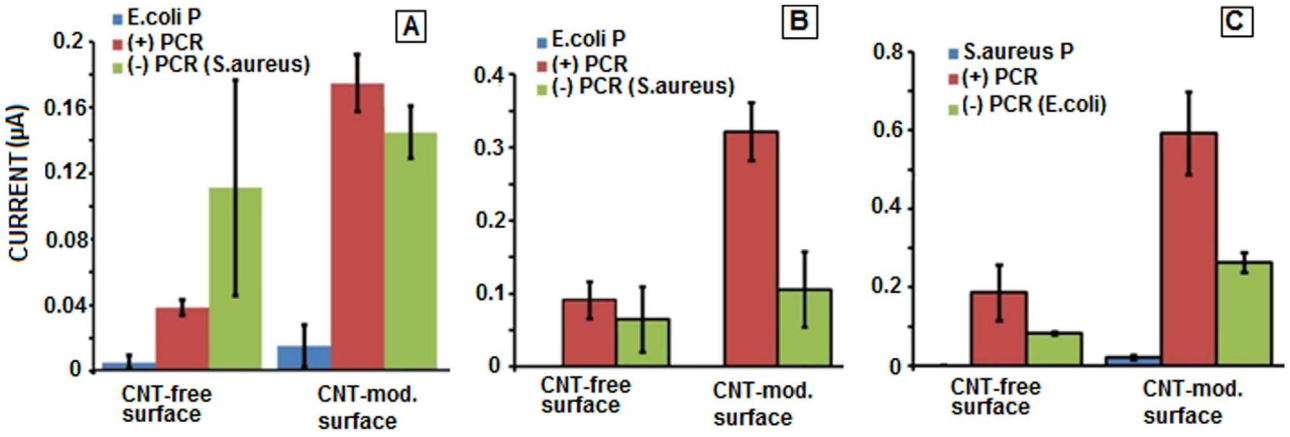

Fig. 6. Histograms show the magnitude of guanine oxidation signals obtained from aPCR samples. Dilution ratio of E. coli aPCR sample is 1:50 (Fig. 6A) or 1:100 (Fig. 6B), and S. aureus is 1:100 (Fig. 6C), respectively. CNT-free sensors were shown as first triple columns (6A, B and C) and probe DNA-wrapped CNT-modified sensor were presented at the second triple columns of the each Fig. (6A–C). Blue columns represent probe, red columns show hybrid, and green columns present noncomplementary signals. Other conditions were shown as Fig. 5. (For interpretation of the references to color in this figure legend, the reader is referred to the web version of this article.)

nanotubes.

The analytical performance of DNA-wrapped single-wall carbon nanotube (SWCNT) immobilized PGE was also tested (Fig. 3, second triple column) in the same experimental conditions with MWCNTs-modified electrode. In comparison to CNTs-free PGE, it showed higher hybridization response than CNTs-free electrode. However, it was seen from Fig. 3 that more stable and reproducible sensor signals were observed when the electrode covered with DNA-wrapped MWCNTs.

A series of three repetitive measurements of the guanine signal related to the synthetic DNA analysis gave reproducible results with RSD of 0.81% for hybrid(main response approximately 2 μA) and 2% for noncomplementary(main response 1.1 μA) sequences (n=3). The guanine oxidation response related to the synthetic hybrid DNA is much more higher than classical hybridization signal that reported in the literature by using PGE and YES/NO detection system [34,39,46,47,50,52–56].

3.4. Detection sensitivity

In Fig. 4, we measured the guanine oxidation signal in response to variable-concentration target such as 7, 10, 12 and 15 μg/mL by using only DNA modified or DNA-wrapped CNTs modified PGE under optimally experimental conditions which were presented in supplementary data from Fig. S2 to S5. The concentration of probe DNA was kept constant at 7 μg/mL (see Fig. S3, Supplementary file).

According to the Fig. 4A, as expected, since capture probe did not include any guanine base, nearly no guanine response was observed in the absence of target DNA. In the presence of full hybridization case, oxidation signals of guanine obtained from target sequences slightly increased in various target concentrations as 7, 10 and 12 μg/mL with both DNA and DNA-wrapped CNTs modified electrode (Fig. 4A, dark violet columns). However, the highest guanine response was observed with a good reproducibility at 12 μg/mL of target concentration (7% of RSD, n=3) by using the nanohybrid modified single-use graphite electrode. Additionally, the DNA-decorated MWCNTs immobilized PGE gave approximately 3.5times more sensitive results compared to only DNA-modified PGE. Upon further increase of target DNA concentration, the guanine signal showed a slight decrease with poor reproducibility because of the saturation of the sensor hybridization sites. Control experiments were performed with a noncomplementary DNA related to the S. aureus genome in the same hybridization conditions (Fig. 4A, white columns).

Using the nanohybrid-modified PGE and based on the guanine signal, the calibration plot was shown in the range of 7–15 μg/mL with error bars (Fig. 4B). The inset figure of the Fig. 4B represented the linear part of the calibration curve and its regression equation (y=0.165x+0.6933) and the R^2 value as 0.9852.

According to the Miller and Miller's method [57] and IUPAC

definition [58] the limit of detection was calculated as 17 nM (equal to 0.5 pmole in 30 μL of reaction volume) with the aid of the linear section of the curve (from 7 to 12 μg/mL) based on this formula:

LOD=3Sb/q.

where Sb is the standard deviation of blank solution (in this study we used the standard deviation of the inosinylated probe DNA signal in the absence of target), q is the slope of the calibration plot.

To our knowledge, the linear part of the curve could be examined for each concentration value as 7, 8, 9, 10, 11 and 12 μg/mL seperately because every value is important in sensitive biosensor applications depending on the surface density, but since the selectivity experiments were also done at the same time with hybridization detection, we have considered values that were presented in Fig. 4.

3.5. The analysis of Typical PCR products

In this study, PCR amplified products were used as "real samples" and their template DNAs were extracted from E. coli or S. aureus bacteria. Fig. 5 presents the detection of real samples (dilution rate 1:50) at CNTs-free or probe DNA-wrapped CNTs modified PGEs. Fig. 5A1 shows the detection of E. coli DNA at CNT-free PGE, 5A2 shows the detection of E. coli DNA with CNTs contained PGE and Fig. 5B1 shows the CNT-free analysis of S. aureus, Fig. 5B2 shows CNT-containing detection of S. aureus respectively. The lowest response was obtained with a guanine-free probe of E. coli or S. aureus (first column of Fig. 5A1, A2, B1 and B2). After the hybridization with denatured positive amplicon, the highest guanine signal was observed (second columns of Fig. 5) with E. coli or S. aureus PCR. When probe DNA bound with noncomplementary real sample, the electrochemical signal showed a significant decrease when it was compared to the hybridization response (third columns of Fig. 5). According to these results, not only CNT-free biosensor but also DNA-wrapped CNT modified genosensor detected the E. coli (Fig. 5A1 and A2) and S. aureus (Fig. 5B1 and B2) bacteria gene regions selectively. However, it was expected to give a higher signal obtained from CNT-contained sensor (Fig. 5A2 and B2) than CNT-free biosensor.

To our knowledge, the observed data can be explained with surface maturation/orientation of PGE. Actually, it should be emphasized that amplification product have a complex matrix that contains primers, dNTPs, enzyme etc. besides thousands of template DNA copies. For this reason, PCR products should be diluted or purified before the hybridization tests. Additionally, denaturation of amplified double-stranded DNA is a critical pretreatment before hybridization between probe and PCR sample. The another effect can be that the saturation of the sensor surface with long PCR sequence causes a higher steric hindrance between probe and amplified product [59] and it is also responsible for the low hybridization response due to re-annealing of both PCR strands [46,60]. To solve renaturation problem, Wang et al. [61] were used "helper oligonucleotide" which was put into denaturation media and it hybridises with one of PCR strand; therefore, target PCR region was keep open by this short sequence for hybridization. This pretreatment step provides sensitive and selective detection of DNA sequences. In the other study, Feriotto et al. [62] reported an analysis procedure that contained asymmetric PCR (aPCR) and they reached highly sensitive and selective detection of hybridization between probe and aPCR sample. Normally, PCR products have a double-stranded DNA structure. Use of a typical PCR product usually causes false positive or negative results in electrochemical analysis because of rapid renaturation of both strands during the experiment [63]. The aPCR methodology generates ssDNA from dsDNA by using the unequal concentrations of forward and reverse primer used in the PCR media. Finally, only one strand of the target DNA sample is preferentially obtained by aPCR technique. Thus, further experiments of this study were carried out with aPCR products.

3.6. The analysis of asymmetric PCR samples

Fig. 6 shows the detection of aPCR samples by using the developed MWCNTs-contained DNA biosensor relies on the DPV transduction of the hybridization reaction between the E. coli probe and its complementary aPCR target or non-complementary sequence (S. aureus aPCR) at different dilution levels as 1:50 (Fig. 6A) and 1:100 (Fig. 6B and C). No electrochemical signal was observed when only probe (P) DNA-wrapped MWCNTs modified PGEs. The appearance of the high guanine signal observed with a positive amplicon that includes target E. coli DNA confirmed the hybridization with PCR product (red columns of Fig. 6). However, when the non-complementary aPCR sample was used as a target during hybridization to confirm of biosensor selectivity, a lower guanine response was observed than the signal of the complementary PCR amplicon (green columns of Fig. 6).

In Fig. 6, the lowest signal was observed with only E. coli (Fig. 6A and B) or S. aureus capture probe (Fig. 6C) modified PGE. E. coli positive aPCR amplicons were shown high guanine signals after the hybridization with E. coli probe wrapped on MWCNTs at PGE surface in both dilution conditions 1:50 and 1:100 (second red columns of Fig. 6A and B). However, the highest hybridization response and the best discrimination rate between fulmatch and non-complementary (S. aureus) aPCR samples were obtained with nanohybrid-modified PGE in 1:100 of dilution rate (second red column of Fig. 6B). Similarly, when the S. aureus capture probe-wrapped MWCNTs-modified electrode hybridized with its complementary aPCR sample, the highest guanine response was observed (second red column of Fig. 6C) and when the S. aureus probe immobilized PGE interacted with noncomplementary (E. coli) sample a significant decrease was observed (second green column of Fig. 6C). With the help of a PBS rinsing step for 5 s with stirring, the effect of nonspecifically adsorbed aPCR samples was minimized.

When we compared guanine signals obtained from Fig. 6A–C based on dilution ratios of aPCR sample, 1:100 of dilution showed better hybridization results (between 350–600 nA, Fig. 6B and C) than the ratio of 1:50 (about 160–180 nA, Fig. 6A) by using CNTs-modified PGEs. When we compared the results of CNTs-free and CNTs-modified sensors, the analytical performance of the DNA-wrapped CNTs-modified transducer gave approximately 3.5 times enhanced hybrid signal with good selectivity and reproducibility for real sample detection when compared with CNTs-free electrode. The reproducibility of the sensor was calculated for three repetitive measurements of guanine responses as relative standard deviations (RSD) of 10.8% for the E. coli positive PCR, 16.9% for the non-complementary S. aureus PCR sample (Fig. 6B), and 16% for the S. aureus positive PCR, 7.2% for the non-complementary E. coli PCR sample (Fig. 6C). Thus, sensitive and reproducible results were obtained with aPCR samples and it is found that more diluted PCR product (1:100) showed higher hybridization efficiency than the concentrated amplicon.

The main hybridization response of the designed sensor for aPCR sample was measured as 350–600 nA which is approximately three times higher than CNTs-free sensor. Besides this, here, it should be emphasized that when we compared this newly-developed PCR-genosensor with our previously reported studies related to real sample analysis, it has DNA-decorated MWCNTs contained surface with lower detection limit and thus it provides more sensitive analysis than the others. For example, Erdem et al. were obtained 150 nA of guanine peak from positive PCR samples with their label-free genomagnetic assay by using PGE [52]. The 120 nA of maximum guanine oxidation signal were observed by Kayran et al. from hybrid DNA by using their kit-type PGE-based genosensor [46]. Ozkan-Ariksoysal et al. also reported 60 nA and 50 nA of guanine signals related to positive PCR products by using PGE and YES/NO detection methodology [34,50]. Thus, in the present study, we reach the highest hybridization response as 350–600 nA by using DNA-wrapped MWCNT and aPCR samples. To our knowledge, the well-organized sensing surface is important to

achieve high and stable sensor responses [46,60]. Thus, the developed protocol provided an effective discrimination between the positive and the negative real samples. To our knowledge, 5 s of simple washing procedure may be improved to obtain better discrimination rate between fullmatch and non-complementary samples by using chemicals such as sodium dodecyl sulphate or Tween 20. However, in our case, we preferred the most simple and rapid way to achieve the difference between positive and negative samples.

Compared to DNA-wrapped CNTs contained studies [20,29,30], our simple and fast method includes real sample analysis for the first time in the literature without using any extra procedure such as magnetic seperation, washing steps, etc. Additionally, no expensive chemicals or electroactive indicator molecule was used for immobilization of CNTs-DNA hybrid onto PGE or monitoring of DNA hybridization. In conclusion, the aPCR application of the modified PGE was explored successfully with this study in 20 min detection time.

4. Conclusions

Our group have initiatively presented the example of using ssDNA-wrapped MWCNTs-modified disposable genosensor for the detection of specific DNA sequences from real samples with the comparison of traditional PCR and aPCR samples for the first time. The ssDNA-MWCNTs nanohybrid structure was immobilized onto the surface of the PGE which is suitable for realizing direct electrochemistry of guanine oxidation. The primary advantage of the developed protocol is its ssDNA-wrapped MWCNTs based detection scheme providing an enhanced signal with high sensitivity. The modification of electrodes provides enhanced adsorption of capture probe onto the electrode surface, and thus they offer approximately three times enhanced sensitivity with low detection limit when compared with CNTs-free sensor. Additionally, in the presence of CNTs, the biosensor reached high detection/discrimination ability with a good reproducibility in 20 min detection time. Another advantage of this biosensor is that its label-free analysis scheme that greatly simplify the sensing procedure by eliminating the use of mediator and the need for the extra experimental step for indicator-DNA interaction. The real sample-contained method is an alternative to the traditional analysis techniques for E. coli detection as the electrophoresis which includes harmful chemicals.

Future direction for this laboratory will be the development of kit-type biosensor [46] containing DNA-decorated CNTs and a device capable of multiple measurements for point-of-care analyses. Because, the use of a CNTs-modified disposable PGE containing the substructure of microarray system, can also enable point-of-care testing in medicine.

Acknowledgments

This work was supported by the Scientific and Technical Research Council of Turkey, TUBITAK, (Project No. 109S263). D.O.-A. and M.O. acknowledge TUBITAK for their financial support. D.O.-A. also acknowledges technical support from the Pharmaceutical Sciences Research Centre (FABAL) of Ege University, Faculty of Pharmacy.

Appendix A. Supporting information

Supplementary data associated with this article can be found in the online version at doi:10.1016/j.talanta.2017.01.005.

References

[1] M. Lazerges, F. Bedioui, Anal. Bioanal. Chem. 405 (2013) 3705–3714.
[2] N. Paniel, J. Baudart, A. Hayat, L. Barthelmebs, Methods 64 (2013) 229–240.
[3] X. Chen, M. Gan, H. Xu, F. Chen, X. Ming, H. Xu, H. Wie, F. Xu, C. Liu, Food Control 46 (2014) 225–232.
[4] S. Agrawal, A. Morarka, D. Bodas, K.M. Paknikar, Appl. Biochem. Biotechnol. 167 (2012) 1668–1677.
[5] R. Singh, M.D. Mukherjeed, G. Sumana, R.K. Gupta, S. Soode, B.D. Malhotra, Sens. Actuators B-Chem. 197 (2014) 385–404.
[6] S.N. Kim, J.F. Rusling, F. Papadimitrakopoulos, Adv. Mater. 19 (2007) 3214–3228.
[7] L. Agui, P. Yanez-Sedeno, J.M. Pingarron, Anal. Chim. Acta 622 (2008) 11–47.
[8] Z. Liu, S. Tabakman, K. Welsher, H.J. Dai, Nano Res. 2 (2009) 85–120.
[9] M. Trojanowicz, TrAC Trends Anal. Chem . 25 (2006) 480–489.
[10] J. Wang, Y.H. Lin, TrAC Trends Anal. Chem. 27 (2008) 619–626.
[11] F. Li, J. Peng, J. Wang, H. Tang, L. Tan, Q. Xie, S. Yao, Biosens. Bioelectron. 54 (2014) 158–164.
[12] K. Umemura, Nanomaterials 5 (2015) 321–350.
[13] E. Katz, I. Willner, ChemPhysChem 5 (2004) 1085–1104.
[14] D. Pantarotto, J.-P. Briand, M. Prato, A. Bianco, Chem. Commun. (2004) 16–17.
[15] M. Zheng, A. Jagota, E.D. Semke, B.A. Diner, R.S. McLean, S.R. Lustig, R.E. Richardson, N.G. Tassi, Nat. Mater. 2 (2003) 338–342.
[16] M. Zheng, B.A. Diner, J. Am. Chem. Soc. 126 (2004) 15490–15494.
[17] N. Nakashima, S. Okuzono, H. Murakami, T. Nakai, K. Yoshikawa, Chem. Lett. 32 (2003) 456–457.
[18] Z. Li, Z. Wu, K. Li, Anal. Biochem. 387 (2009) 267–270.
[19] S. Malik, S. Vogel, H. Rosner, K. Arnold, F. Hennrich, A.-K. Köhler, C. Richert, M.M. Kappes, Compos. Sci. Technol. 67 (2007) 916–921.
[20] N.T. Thuy, P.D. Tama, M.A. Tuan, A.-T. Le, L.T. Tama, V.V. Thu, N.V. Hieu, N.D. Chien, Curr. Appl. Phys. 12 (2012) 1553–1560.
[21] J.M. Hughes, H. Cathcart, J.N. Coleman, J. Phys. Chem. C 114 (2010) 11741–11747.
[22] P.G. He, M. Bayachou, Langmuir 21 (2005) 6086–6092.
[23] W. Yan, X.C. Shen, Z.L. Zhang, C. Chen, D.W. Pang, Anal. Lett. 38 (2005) 2579–2595.
[24] S.S.J. Aravind, S. Ramaprabhu, Sens. Actuators B 155 (2011) 679–686.
[25] S.R. Cao, J.F. Wang, R. Yuan, Y.Q. Chai, Sens. Lett. 9 (2011) 1636–1642.
[26] J. Shi, T.G. Cha, J.C. Claussen, A.R. Diggs, J.H. Choi, D.M. Porterfield, Analyst 136 (2011) 4916–4924.
[27] L. Zhang, C.Z. Huang, Y.F. Li, S.J. Xiao, J.P. Xie, J. Phys. Chem. B 112 (2008) 7120–7122.
[28] R.M. Williams, S. Nayeem, B.D. Dolash, L.J. Sooter, PLoS One 9 (2014) e94117.
[29] X. Zhang, K. Jiao, S. Liu, Y. Hu, Anal. Chem. 81 (2009) 6006–6012.
[30] H. Nie, Z. Yang, S. Huang, Z. Wu, H. Wang, R. Yu, J. Jiang, Small 8 (2012) 1407–1414.
[31] G.C. Baker, J.J. Smith, D.A. Cowan, J. Microbiol. Methods 55 (2003) 541–555.
[32] K. Watanabe, Y. Kodama, S. Harayama, J. Microbiol. Methods 44 (2001) 253–262.
[33] F. Martineau, F.J. Picard, P.H. Roy, M. Ouellette, M.G. Bergeron, J. Clin. Microbiol. 36 (1998) 618–623.
[34] D. Ozkan-Ariksoysal, B. Tezcanli, B. Kosova, M. Ozsoz, Anal. Chem. 80 (2008) 588–596.
[35] M. Yang, M.E. McGovern, M. Thompson, Anal. Chim. Acta 346 (1997) 259–275.
[36] T. Hertel, R.E. Walkup, P. Avouris, Phys. Rev. B 58 (1998) 13870–13873.
[37] T. Gu, Y. Zhang, F. Deng, J. Zhang, Y. Hasebe, J. Environ. Sci. 23 (Supplement) (2011) S66–S69.
[38] J. Li, Q. Liu, Y. Liu, S. Liu, S. Yao, Anal. Biochem. 346 (2005) 107–114.
[39] A. Erdem, M. Muti, H. Karadeniz, G. Congur, E. Canavar, Colloid Surf. B 95 (2012) 222–228.
[40] A.A. Ensafi, M. Amini, B. Rezaei, Colloid Surf. B 109 (2013) 45–51.
[41] L.M. Bravo-Anaya, J.F.A. Solteroa, M. Rinaudo, Int. J. Biol. Macromol. 88 (2016) 345–353.
[42] S. Jung, M. Cha, J. Park, N. Jeong, G. Kim, C. Park, J. Ihm, J. Lee, J. Am. Chem. Soc. 132 (2010) 10964–10966.
[43] W.S. Choi, S.H. Choi, B. Hong, D.G. Lim, K.J. Yang, J.H. Lee, Mater. Sci. Eng. C 26 (2006) 1211–1214.
[44] A. Erdem, P. Papakonstantinou, H. Murphy, Anal. Chem. 78 (2006) 6656–6659.
[45] I.D. Rosca, F. Watari, M. Uo, T. Akasaka, Carbon 43 (2005) 3124–3131.
[46] Y.U. Kayran, D. Ozkan-Ariksoysal, B. Tezcanli, B. Kosova, M. Ozsoz, Electroanalysis 25 (2013) 2668–2676.
[47] D. Ozkan, A. Erdem, P. Kara, K. Kerman, B. Meric, J. Hassmann, M. Ozsoz, Anal. Chem. 74 (2002) 5931–5936.
[48] B. Meric, K. Kerman, D. Ozkan, P. Kara, M. Ozsoz, Electroanalysis 14 (2002) 1245–1250.
[49] S.N. Topkaya, D. Ozkan-Ariksoysal, Electroanalysis 28 (2016) 1077–1084.
[50] D.O. Ariksoysal, H. Karadeniz, A. Erdem, A. Sengonul, A.A. Sayiner, M. Ozsoz, Anal. Chem. 77 (2005) 4908–4917.
[51] Z. Zhang, C. Shen, M. Wang, H. Han, X. Cao, BioTechniques 44 (2008) 537–545.
[52] A. Erdem, D.O. Ariksoysal, H. Karadeniz, P. Kara, A. Sengonul, A.A. Sayiner, M. Ozsoz, Electrochem. Commun. 7 (2005) 815–820.
[53] T. Kilic, S.N. Topkaya, D. Ozkan-Ariksoysal, M. Ozsoz, P. Ballar, Y. Erac, O. Gozen, Biosens. Bioelectron. 38 (2012) 195–201.
[54] G. Gokce, A. Erdem, C. Ceylan, M. Akgöz, Talanta 149 (2016) 244–249.
[55] M. Muti, S. Sharma, A. Erdem, P. Papakonstantinou, Electroanalysis 23 (2011) 272–279.
[56] A. Erdem, P. Papakonstantinou, H. Murphy, M. McMullan, H. Karadeniz, S. Sharma, Electroanalysis 22 (2010) 611–617.
[57] J.N. Miller, J.C. Miller, Statistics and Chemometrics for Analytical Chemistry, 5th ed., Pearson Education, Essex, UK, 2005, pp. 121–123.
[58] J. Mocak, A. Bond, S. Mitchell, G. Scollary, Pure Appl. Chem. 69 (1997) 297–328.
[59] G. Marrazza, G. Chiti, M. Mascini, M. Anichini, Clin. Chem. 46 (2000) 31–37.
[60] F. Lucarelli, G. Marrazza, A.P.F. Turner, M. Mascini, Biosens. Bioelectron. 19 (2004) 515–530.
[61] R.H. Wang, M. Minunni, S. Tombelli, M. Mascini, Biosens. Bioelectron. 20 (2004) 598–605.
[62] G. Feriotto, M. Lucci, N. Bianchi, C. Mischiati, R. Gambari, Hum. Mutat. 13 (1999) 390–400.
[63] L.L. Li, H. Cai, T.H. Lee, J. Barfood, I.M. Hsing, Electroanalysis 16 (2004) 81–87.